What Level of Accuracy Is Achievable for Preclinical Dose Painting Studies on a Clinical Irradiation Platform?

Authors: Trani, Daniela, Reniers, Brigitte, Persoon, Lucas, Podesta, Mark, Nalbantov, Georgi, et al.

What Level of Accuracy Is Achievable for Preclinical Dose Painting Studies on a Clinical Irradiation Platform?

Daniela Trani,[a,1] Brigitte Reniers,[a,b] Lucas Persoon,[a] Mark Podesta,[a] Georgi Nalbantov,[a] Ralph T. H. Leijenaar,[a] Marlies Granzier,[a] Ala Yaromina,[a] Ludwig Dubois,[a] Frank Verhaegen[a,c,2] and Philippe Lambin[a,2]

[a] *Maastricht Radiation Oncology (MAASTRO), GROW - School for Oncology and Developmental Biology, Maastricht University Medical Centre, Maastricht, The Netherlands;* [b] *Research Group NuTeC, CMK, Hasselt University, Agoralaan Gebouw H, B-3590 Diepenbeek, Belgium; and* [c] *Medical Physics Unit, Department of Oncology, McGill University, Montréal, Québec H3G 1A4, Canada*

Trani, D., Reniers, B., Persoon, L., Podesta, M., Nalbantov, G., Leijenaar, R. T. H., Granzier, M., Yaromina, A., Dubois, L., Verhaegen, F. and Lambin, P. What Level of Accuracy is Achievable for Preclinical Dose Painting Studies on a Clinical Irradiation Platform? *Radiat. Res.* **183, 501–510 (2015).**

Advancements made over the past decades in both molecular imaging and radiotherapy planning and delivery have enabled studies that explore the efficacy of heterogeneous radiation treatment ("dose painting") of solid cancers based on biological information provided by different imaging modalities. In addition to clinical trials, preclinical studies may help contribute to identifying promising dose painting strategies. The goal of this current study was twofold: to develop a reproducible positioning and set-up verification protocol for a rat tumor model to be imaged and treated on a clinical platform, and to assess the dosimetric accuracy of dose planning and delivery for both uniform and positron emission tomography-computed tomography (PET-CT) based heterogeneous dose distributions. We employed a syngeneic rat rhabdomyosarcoma model, which was irradiated by volumetric modulated arc therapy (VMAT) with uniform or heterogeneous 6 MV photon dose distributions. Mean dose to the gross tumor volume (GTV) as a whole was kept at 12 Gy for all treatment arms. For the nonuniform plans, the dose was redistributed to treat the 30% of the GTV representing the biological target volume (BTV) with a dose 40% higher than the rest of the GTV (GTV – BTV) (~15 Gy was delivered to the BTV vs. ~10.7 Gy was delivered to the GTV – BTV). Cone beam computed tomography (CBCT) images acquired for each rat prior to irradiation were used to correctly reposition the tumor and calculate the delivered 3D dose. Film quality assurance was performed using a water-equivalent rat phantom. A comparison between CT or CBCT doses and film measurements resulted in passing rates >98% with a gamma criterion of 3%/2 mm using 2D dose images. Moreover, between the CT and CBCT calculated doses for both uniform and heterogeneous plans, we observed maximum differences of <2% for mean dose to the tumor and mean dose to the biological target volumes. In conclusion, we have developed a robust method for dose painting in a rat tumor model on a clinical platform, with a high accuracy achieved in the delivery of complex dose distributions. Our work demonstrates the technical feasibility of this approach and enables future investigations on the therapeutic effect of preclinical dose painting strategies using a state-of-the-art clinical platform. © 2015 by Radiation Research Society

INTRODUCTION

Although recent evidence suggests that intratumor biological heterogeneity plays an important role in the treatment failure of solid cancers (*1, 2*), radiotherapy is still based on delivering uniform doses to the treatment target. Several biological factors, such as tumor hypoxia, glucose metabolism and perfusion, have been shown to correlate with radiotherapy outcome (*3, 4*), and noninvasive imaging techniques, such as positron emission tomography (PET), can be used to assess their distribution across the tumor bulk. The potentially radioresistant subvolumes identified by molecular imaging, also referred to as biological target volumes (BTVs), may require higher radiation doses to achieve tumor control than the rest of the gross tumor volume (GTV) (*5, 6*).

The integration of intratumor biological heterogeneity maps into modern radiotherapy techniques, such as volumetric modulated arc therapy (VMAT), generates a molecular imaging-based dose painting in which the radiation dose to the BTVs is increased by redistributing or escalating the total dose across the tumor (*7, 8*). The hypothesis that PET-based heterogeneous irradiation of solid cancers might lead to better tumor control compared to standard uniform irradiation has been tested mainly by modeling studies (*9, 10*). A limited number of clinical trials have also been performed (*11*) or are currently ongoing (*12, 13*). Preclinical studies might be important, together with

501

clinical trials, for testing of complex radiobiological hypotheses and dose painting strategies (*14, 15*). Currently, dose painting is beyond the capabilities of treatment planning systems (TPS) for small animal radiotherapy, although novel equipment for precision irradiation is already available (*16*). The goal of this study was twofold: to develop a robust positioning and set-up verification protocol, and to assess feasibility as well as dosimetric accuracy for PET-based dose painting in a rat tumor model using state-of-the-art clinical imaging and radiotherapy platforms.

MATERIALS AND METHODS

Workflow

The experimental set-up for preclinical ^{18}F-deoxyglucose (FDG) PET-CT-guided radiotherapy in rats is made up of the following steps:

1. Injection of FDG [time for optimal uptake is 2 h (*17*)];
2. Rat positioning and PET-CT image acquisition;
3. PET and CT image segmentation to identify target structures and organs at risk (OARs) for the treatment plan;
4. Design and optimization of the treatment plan;
5. Repositioning of the rat on the clinical accelerator;
6. CBCT image acquisition;
7. CBCT to CT image matching;
8. Radiation dose delivery.

Animal Model

Adult male WAG/Rij rats were implanted subcutaneously with syngeneic R1 rhabdomyosarcomas ($\sim$1 mm^3) in the left flank as described previously (*18*). The radiosensitivity of this tumor model is well known (*19, 20*), and both the size and biological intratumor heterogeneity of the lesions (*18*) make it suitable for our study purposes. All animal procedures and experiments were approved by the Animal Ethical Committee of Maastricht University (2012-009). At an average tumor volume of 7.5 $\pm$ 0.9 cm^3, animals (n = 9) were included in the experiment described in the above section: *Workflow*.

Buildup Bolus

Due to the small size of tumor-bearing rats, the use of a buildup bolus is needed to optimally shape the dose distribution to the target for MV photon beams. Throughout our study, we used a 1 cm thick Super Stuff® bolus (no. 489-050, Radiation Products Design Inc., Albertville, MN).

CT Hounsfield Units to Electron Densities Conversion and CBCT Calibration

To ensure accurate dose calculations for both CT-based treatment planning and CBCT-based dose calculations, well-characterized Hounsfield units to electron density (HU-to-ED) calibration curves were needed. For this characterization, we used a rat-size phantom with densities equivalent to heterogeneous clinical phantoms (Supplementary Fig. S1; http://dx.doi.org/10.1667/RR13933.1.S1) and an imaging protocol of 100 kV and 73.5 mAs (for more details see Supplementary Methods; http://dx.doi.org/10.1667/RR13933.1.S1).

PET-CT Imaging and Contouring

Animals were injected with 21.2 $\pm$ 2.1 MBq [^{18}F]FDG, 2 h after the injection, while sedated [100 mg/kg ketamine and 10 mg/kg xylazine (intraperitoneal)] were placed on the support table of a clinical PET/CT Biograph™ scanner [SOMATOM TruePoint™ Sensation-40 with an ECAT® ACCEL™ PET scanner; Siemens, Erlangen, Germany (CT: 120 kVp/170 mAs, 1 mm slice thickness)]. Prior to scanning, alignment was performed with the laser guides, and cross hairs were drawn with skin ink on areas of the body where the fur had been removed (Supplementary Fig. S2; http://dx.doi.org/10.1667/RR13933.1.S1). The bolus was placed around the animal to surround the tumor completely (Supplementary Fig. S3A; http://dx.doi.org/10.1667/RR13933.1.S1). While one operator placed the free end of the bolus (from left to right in Supplementary Fig. S3A and B) around the anaesthetized animal, another operator gently held the animal so that the body would not be displaced during bolus positioning. Each animal was scanned individually. The PET/CT Biograph scanner had an axial field of view (FoV) of 162 mm, a transaxial FoV of 605 mm and a spatial resolution of 5.3 mm FWHM at the center of the FoV. Attenuation correction of the PET data was performed using the acquired CT images. The acquisition of a topogram was followed by a whole-body CT scan using a 1 mm reconstructed slice thickness and a pitch of 0.8. Immediately after the CT scan, a dynamic emission scan in list mode (LM) was started for 20 min in one bed position. Afterward, LM data were resampled using Fourier rebinning and PET image reconstruction was performed. For GTV contouring and FDG-uptake-based BTV segmentation, the PET-CT scan was imported into the image processing software Imalytics Research Workstation (Philips GmbH, Innovative Technologies, Aachen, Germany). The GTV on the CT scan (GTV contours on CT images hereafter referred to as GTV1) was manually delineated. The FDG high-uptake region (BTV$_{high}$) was defined as the 30% of the GTV1 characterized by the highest standard uptake value (SUV). Similarly, the FDG low-uptake region inside the GTV1 (BTV$_{low}$) was defined as the 30% of the GTV characterized by the lowest FDG SUV. This SUV-based volume thresholding was performed with Imalytics software using a semi-manual process to search for the SUV value, which would identify the desired BTV within the contoured GTV. The GTV1 and BTV contours were sent to the Eclipse™ TPS (Varian Medical Systems, Palo Alto, CA) together with the CT images and were used for treatment planning. The animal body and spine in the treatment field were segmented automatically, while the abdominal region containing the gastrointestinal tract was manually delineated.

Assessment of the In Vivo Accuracy in Repositioning between CT and CBCT Scans

On the same day of the PET-CT scan, animals were individually repositioned on the treatment couch, and each underwent animal and tumor alignment, as described in the previous section. A CBCT scan was then acquired with the linac's on-board imager (TrueBeam™ STx High-Definition 120 Multileaf, Varian Medical Systems) and registered to the pretreatment CT scan. Matching of CBCT to planning CT scan was manually performed and evaluated on the basis of a 3D visual inspection performed primarily on the GTV. When no acceptable CBCT to CT tumor matching could be achieved by shifting the treatment table in the four available degrees of freedom (translations along all three axes and rotations along the axis perpendicular to the treatment couch), we repositioned the animal and the tumor again and acquired a new CBCT. The sequence was iterated until an acceptable online matching between CBCT and CT was obtained. Upon successful completion of CBCT to CT online matching, the GTV was manually delineated offline on the CBCT scan (GTV contours on CT images are referred to as GTV2). To quantify the accuracy of the CBCT to CT matching, we calculated the value of the Dice similarity coefficient (DSC), defined as:

$$DSC = 2 \times \frac{GTV1 \cap GTV2}{GTV1 + GTV2}. \tag{1}$$

Treatment Planning

Animals were randomly assigned (n = 3 per group) to one of the following treatment arms: A. standard uniform dose distribution to GTV1; B. dose redistribution with the BTV_{high} to receive a 40% higher dose than the rest of GTV1 (GTV1 – BTV); or C. dose redistribution with the BTV_{low} to receive a 40% higher dose than GTV1 – BTV. The mean dose (D_{mean}) to GTV1 was maintained at 12 Gy for all treatment groups. For uniform plans, RapidArc VMAT treatment plans were created [Acuros XB algorithm (Eclipse ver. 10)] that employed a single full 360° arc. For BTV_{high} and BTV_{low} boost plans, two full arcs were required to produce an optimal dose distribution. Dose calculations were performed using the smallest possible grid size (0.1 cm).

Quantification of Discrepancies between Planned vs. Prescribed Doses to Target Structures

For any given target structure, an absolute dose difference image (ΔD) was determined, where ΔD (x) represents the absolute dose difference in voxel x, defined as:

$$\Delta D\,(x) = |D_{pres}(x) - D_{plan}(x)|, \qquad (2)$$

where D_{pres} is the prescribed and D_{plan} the CT-planned dose image. We calculated mean and standard deviation of ΔD, $\Delta D_{5\%}$ and $\Delta D_{95\%}$, where 95% and 5% of the structure volume will have an absolute dose discrepancy (in Gy) of less than $\Delta D_{5\%}$ and $\Delta D_{95\%}$, respectively. We computed the dose discrepancy for the GTV1 contour in the case of uniform treatment plans, and for the GTV1, $BTV_{high/low}$ and GTV1 – $BTV_{high/low}$ contours in the case of heterogeneous treatment plans. We compared the mean ΔD between treatment arms for each target structure using a Kruskal-Wallis one-way analysis of variance by ranks.

Comparison between CT-Planned and CBCT-Recalculated Dose Distributions

For each animal, a retrospective structure-based comparison was performed between planned doses using the CT and CBCT images. We created a new structure set on the CBCT scan of each animal that included a copy of GTV1 and a copy of BTV. The plan was then recalculated on the CBCT scan using an appropriate HU-to-ED calibration curve (Supplementary Methods and Figures S1–S6; http://dx.doi.org/10.1667/RR13933.1.S1). Next, the CT and CBCT calculated 3D doses were compared on the basis of several dose volume histogram (DVH) metrics (Table 5). For one case of CT and CBCT, calculated doses were also compared with a 3D gamma analysis (*21*, *22*).

EBT3 Film Dosimetry

Assessment of dosimetric accuracy was performed by comparing planar slices of the dose distributions calculated in the Eclipse for uniform and heterogeneous RapidArc plans to radiochromic film measurements. For the dosimetrical study, we used an in-house fabricated water-equivalent wax phantom with the approximate shape and size of a rat bearing a large subcutaneous flank tumor (Fig. 1A). The phantom was made of two water-equivalent slabs (Fig. 1B) (bottom slab thickness: ~16.07 ± 0.01 mm; top slab thickness: ~21.20 ± 0.01 mm). Laser cross hairs were used to position the phantom, and corresponding marking lines were drawn with a marker pen on the inside of the bottom slab (Fig. 1B). Metallic spherical X-ray markers (d = 1.5 mm, SL-15, SureMark®) were also included in the top and bottom slabs (Fig. 1C) to serve as guides during CT to CBCT scan matching before film irradiation. A ~1 cm thick Super Stuff bolus was used to surround the wax phantom both at the time of CT and CBCT scanning as well as during irradiation (Supplementary Fig. S4B; http://dx.doi.org/10.1667/RR13933.1.S1). The CT scan of the wax phantom was imported into Eclipse and used to create verification plans for four different rat plans (n = 1 for the uniform arm; n = 2 for the BTV_{low} boost arm; n = 1 for the BTV_{high} boost arm). For each verification plan, the phantom CT image was registered offline to the rat CT image so that the rat tumor was centered to the homologous region of the phantom. The rat VMAT plan was then copied to the phantom CT and the 3D dose recalculation was performed. Next, the phantom was repositioned on the treatment couch and a CBCT scan was acquired and matched to the CT scan using the position of the X-ray markers as a 3D reference. Gafchromic EBT3 films (lot no. A05021301; Ashland Specialty Ingredients, Wayne, NJ) were cut into approximately 8×8 cm^2 pieces shaped to the tumor and placed inside the wax phantom after matching the CBCT to the pretreatment CT. EBT3 films were calibrated between 0 and 2,400 cGy with an Expression® 10000XL flatbed scanner (Epson® America Inc., Long Beach, CA) (*23*). For all four plans, the online matched CBCT was used to recalculate the 3D doses. Agreement between the film measurements and the CT- or CBCT-TPS calculated doses was assessed using 2D gamma analysis (FilmQA™ Pro, Ashland Specialty Ingredients).

RESULTS

Accuracy of In Vivo Tumor Repositioning

After matching the GTV2 (CBCT) to the GTV1 (CT), we observed that tumor/animal and bolus were correctly repositioned after the first CBCT scan, occasionally requiring more than one scan for satisfactory matching of CT and CBCT images (Table 1). Only for the rat with identification (ID) number 3, three CBCT scans were acquired before an acceptable matching was achieved (Table 1). Figure 2 shows a representative example of the quality of CBCT to CT matching achieved with our protocol: the contours of the GTV delineated on the CT (Fig. 2A) (blue contour) and on the CBCT (Fig. 2B) (red contour) strongly overlapped, and the thickness of the Super Stuff bolus at different positions remained nearly constant throughout the entire experiment. We estimated the conformity of CBCT to CT scan for each animal offline by calculating the corresponding DSC values for the GTV1 and GTV2 contours (Table 1). The DSC was >0.9 for all animals (range: 0.90–0.98) included in this study. As shown in Fig. 2, while an excellent matching of the tumor could be achieved, the matching of the bony structures was often suboptimal. This is due to the high flexibility that characterizes rats as well as other rodents.

Quantification of Discrepancies between Planned vs. Prescribed Doses to Target Structures

The characteristics of the nine different rat tumors and target structures included in this study are reported in Table 2. The GTV1 was 11.0 ± 1.5 cm^3 (9.4–14.2 cm^3) on average. The BTV fractional size was 30.6% of the GTV on average, ranging from 27.8 to 33.6% of the GTV1. Details on the dose metrics prescribed for uniform and heterogeneous treatments (BTV_{high} and BTV_{low}) are provided in Table 3. The mean and standard deviation of ΔD as well as $\Delta D_{5\%}$ and $\Delta D_{95\%}$ for GTV1, BTV and GTV1 – BTV are given in Table
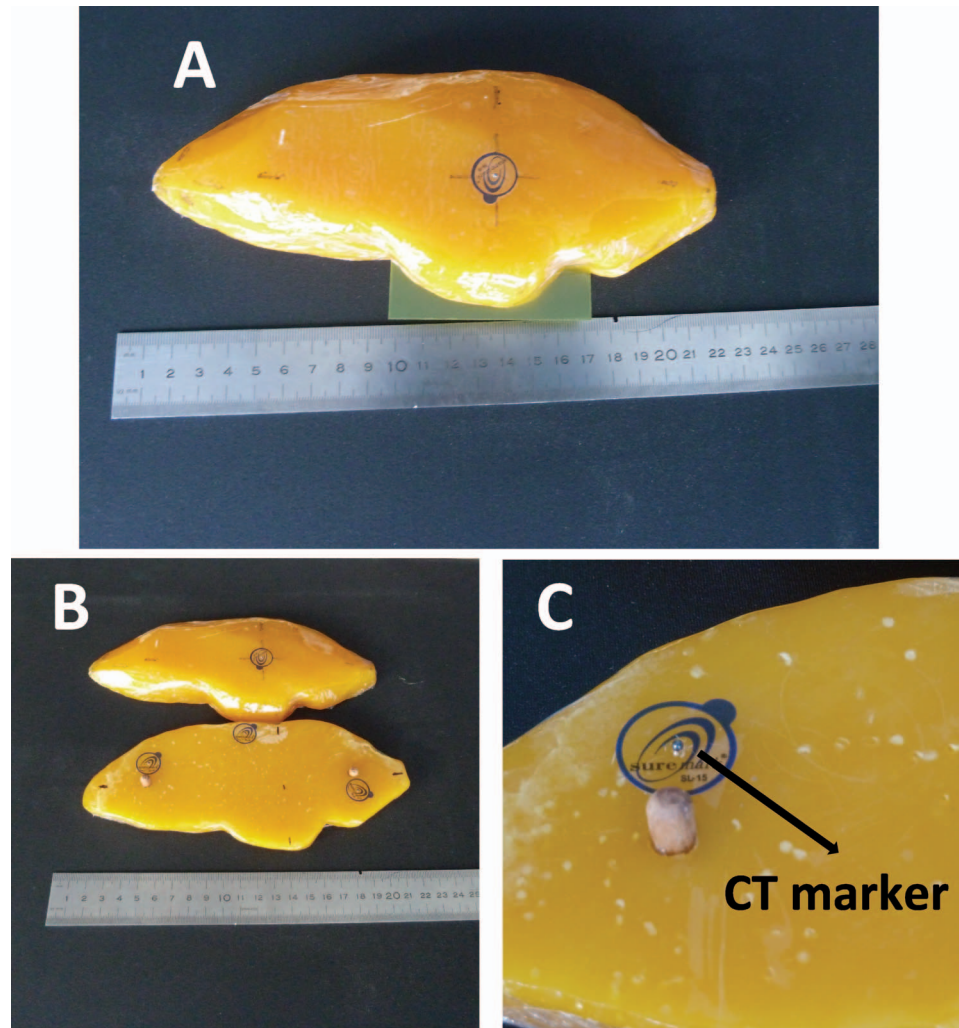
FIG. 1. In-house fabricated water-equivalent phantom (panel A) resembling in both size and shape a rat carrying a flank tumor. In its inside an EBT3 film is visible. The phantom was made of two slabs (panel B); the phantom was equipped with ball CT markers (panel C) for CBCT to CT matching.

4. The mean ΔD within the entire GTV1 was found to be lower for the uniform treatment plans ($P = 0.03$), compared to the two boost arms, and was always smaller than 2% of the prescribed mean tumor dose. There was no significant difference in the mean ΔD between the two boost arms (Fig. 3A). The mean ΔD within the BTV was lower for the BTV_{high} boost treatment arm, compared to the BTV_{low} boost arm ($P = 0.025$) (Fig. 3B). For the GTV1 – BTV structure, there was no significant difference in the mean ΔD between the two boost treatment arms ($P = 0.138$) (Fig. 3C). $\Delta D_{5\%}$ values suggest that the highest dose discrepancies within the GTV were mainly located in the GTV1 – BTV subvolume for the nonuniform treatment arms.

Comparison between CT-Planned and CBCT-Recalculated Dose Distributions

For each treatment arm, an example of 2D dose distribution is shown in Fig. 4. The DVH metrics for both CT and CBCT doses are reported in Table 5. As shown in the nonuniform plans in Table 5, to achieve full coverage of the BTV regions, we had to pull up the dose in the GTV1 – BTV, leading to slightly greater mean doses to the entire GTV1. The DVH metrics $D_{95\%}$ and $D_{5\%}$ for GTV1 were stable between CT and CBCT, with differences <1 and <2.5%, respectively, regardless of treatment type and tumor size. Only for the rat no. 9, included in the BTV_{low} arm, the GTV1 $D_{5\%}$ calculated on the CBCT was 8% lower than in the CT dose volume. The dose difference for GTV1 D_{mean}, GTV1 D_{min}, BTV $D_{5\%}$ and BTV D_{min} were always <2%, regardless of the treatment type. For one case (rat no. 1), CT and CBCT calculated doses were also compared with a 3D gamma analysis (single slice shown, Supplementary Fig. S5; http://dx.doi.org/10.1667/RR13933.1.S1).

Assessment of Dosimetric Accuracy for Uniform and Boost Plans

The CT- and CBCT-TPS-calculated dose distributions were compared to radiochromic film measurements by

TABLE 1
Dice Similarity Coefficients (DSC) for Matching of CBCT to CT Scan of Rat Rhabdomyosarcomas

Rat no.	GTV1 (cm³)	GTV2 (cm³)	DSC	Number of CBCT scans
1	9.4	8.7	0.90	1
2	11.3	10.0	0.93	1
3	10.0	9.5	0.93	3
4	10.8	11.2	0.98	1
5	11.3	11.0	0.93	1
6	10.0	10.0	0.93	1
7	12.5	12.5	0.94	1
8	14.2	14.0	0.96	1
9	9.7	9.4	0.93	1

Note. GTV1 = gross tumor volume delineated on planning CT; GTV2 = gross tumor volume delineated on CBCT image.

performing a gamma analysis on 2D dose images. All passing rates with a 3%/2 mm criterion were >98% (Table 6), which indicated a high accuracy in dose delivery for both uniform and heterogeneous dose prescriptions, regardless of the treatment type.

DISCUSSION

It has been suggested, based on several clinical studies, that high intratumoral uptake of FDG or hypoxia PET tracers might potentially identify radioresistant subregions in solid cancers, and that targeting these biological volumes with higher radiation doses might lead to improved tumor control in radiotherapy patients compared to standard uniform dose distributions (*8, 24, 25*). A variety of dose painting approaches can be developed for boost or dose-redistribution treatment, and they can be based on the (combined) use of different PET tracers. Although some are already being utilized in clinical trials, preclinical studies in rodent models might nevertheless be of great value in exploring and selecting treatment strategies to be tested in human trials. Dedicated small animal radiotherapy platforms are now available at several institutions. This is considered a major technological advancement for precision radiation preclinical studies. However, until recently the major technological bottleneck in preclinical radiotherapy has been the lack of a dedicated TPS for small animals. A TPS that allows for preclinical image-guided radiotherapy (IGRT) has been recently developed (*26*), however, more work in this area is needed to enable the delivery of complex dose distributions to rodent tumor models using dedicated imaging and irradiation platforms (*16, 27*). In this study we developed a robust positioning and set-up verification protocol, and assessed feasibility and dosimetric accuracy for preclinical PET-based dose painting studies using state-of-the-art clinical imaging and irradiation platforms. We employed a rat tumor model that, due to its physical and biological characteristics, appears suitable for this type of preclinical investigations.

As our study was performed on a clinical platform, we had to take into account that when using MV photon beams a build-up bolus is needed to optimally shape the dose distribution to the rat tumor. Super Stuff bolus (*28*) met three essential requirements for high throughput preclinical
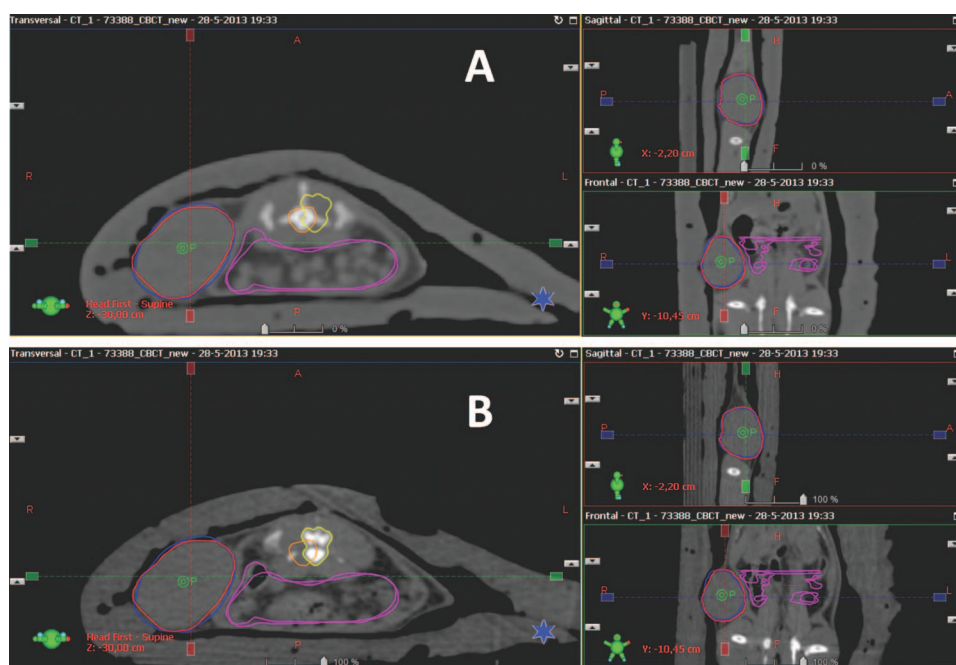

FIG. 2. Example of matched CT (panel A) and CBCT (panel B) images for a rat with a flank tumor. The GTV contoured on the CT image is in blue in both images; the contour of the GTV re-delineated on the CBCT is shown in red. The thickness (~1 cm) and position of the Super Stuff bolus, visible as the structure surrounding the animal's body, are consistent between CT and CBCT.

TABLE 2
GTV1 and BTV Characteristics for Rat Tumors Planned to Receive 12 Gy as a Uniform Dose or Dose Redistributed to Boost the BTV$_{high}$ or BTV$_{low}$ Tumor Subvolumes

Rat no.	Treatment type	GTV1 (cm³)	BTV (cm³)	GTV1 ∩ BTV (%)	Mean GTV1 SUV (±SD)	Minimum GTV1 SUV	Maximum GTV1 SUV	Mean BTV SUV (±SD)	Minimum BTV SUV	Maximum BTV SUV
1	Uniform	9.4	N/A	N/A	1.9 ± 0.8	0.17	3.59	N/A	N/A	N/A
2	Uniform	11.3	N/A	N/A	2.2 ± 1.0	0.17	4.13	N/A	N/A	N/A
3	Uniform	10.0	N/A	N/A	0.4 ± 0.7	0.00	3.17	N/A	N/A	N/A
4	BTV$_{high}$ boost	10.8	3.0	27.5	2.3 ± 1.0	0.29	4.59	3.6 ± 0.4	2.21	4.59
5	BTV$_{high}$ boost	11.3	3.8	33.3	1.9 ± 0.9	0.24	4.23	2.9 ± 0.5	1.22	4.23
6	BTV$_{high}$ boost	10.0	3.1	36.6	1.7 ± 0.8	0.10	3.17	2.6 ± 0.3	1.31	3.17
7	BTV$_{low}$ boost	12.5	4.0	32.0	2.3 ± 1.1	0.15	4.67	1.2 ± 0.5	0.15	3.41
8	BTV$_{low}$ boost	14.2	4.2	29.2	2.5 ± 1.3	0.10	6.06	1.2 ± 0.6	0.10	6.06
9	BTV$_{low}$ boost	9.7	2.9	29.9	4.2 ± 2.1	0.17	8.25	1.9 ± 0.9	0.17	8.25

Note. GTV1 = gross tumor volume delineated on planning CT; BTV = biological target volume delineated on pretreatment ^{18}F-deoxyglucose (FDG) PET; SD = standard deviations of the mean; SUV = standardized uptake value.

dose painting studies: 1. Ease of preparation; 2. Ability to maintain a reproducible thickness and shape throughout the experiment; and 3. Ability to conform well to the tumor and animal body shape to minimize air gaps at the interfaces.

The first major challenge for radiation dose painting studies is repositioning of the tumor and the animal correctly at the time of treatment, so that the plan designed on the pretreatment scan is delivered correctly on the treatment table. Our repositioning protocol resulted in an excellent matching between CT- and CBCT-delineated target structures. While differences in tumor contouring between CT and CBCT were negligible in our tumor model, these differences might become important when employing tumors with smaller sizes due to imaging artifacts. Although all cases reported were characterized by an accurate CBCT to CT tumor matching, poor registration might occur occasionally between the two images, due to suboptimal animal/tumor repositioning. In these cases, as in the case of radiotherapy patients, the availability of online correction tools and strategies would be highly valuable. It is also important to consider that our TrueBeam linac allows us to perform shifts using only four degrees of freedom, and that easier matching between CBCT and CT images can be obtained on versions where the couch is equipped with six degrees of freedom. Other intrinsic limitations of our approach worth noting are the relatively low-PET resolution, the manual segmentation of target structures, and the manual registration between CT and CBCT images. Higher PET resolution and automation of matching and delineation would reduce segmentation and registration uncertainties.

Our group recently reported that FDG-PET uptake in the rat rhabdomyosarcomas is highly stable for at least 6 h and that even comparison between scans acquired 48 h apart leads to a good overlap of BTVs (*17*). In the current study, we propose a workflow where an FDG-PET-CT scan is acquired prior to planning and a CBCT to CT tumor-based match is performed immediately before treatment, on the same day of planning. In this way, we can assume that the BTV has remained acceptably stable and that a tumor-based match will also in general correspond to a BTV match. Unlike in human patients, in rodents a matching based on bony structures often leads to inaccurate tumor match due to the high flexibility of these animals. For this reason we chose to always adopt only a CBCT to CT tumor-based match.

When planning and performing preclinical dose painting studies on clinical platforms, uncertainty in repositioning and MV beam characteristics (including width of the beam

TABLE 3
Prescribed Dose Parameters for Uniform, BTV$_{high}$ and BTV$_{low}$ Boost

Structure	Optimization objective	Uniform (arm A) dose objective (Gy)	BTV$_{high}$ boost (arm B) dose objective (Gy)	BTV$_{low}$ boost (arm C) dose objective (Gy)
GTV1	D$_{Mean}$	12	12	12
GTV1	Minimum D$_{99}$	≥10.8 (90% D$_{Mean}$)	Minimum D$_{99GTV - BTV}$	Minimum D$_{99GTV - BTV}$
GTV1	D$_{Max}$	≤13.2 (110% MDT)	D$_{MaxBTV}$	D$_{MaxBTV}$
BTV	D$_{MeanBTV}$	N/A	15	15
BTV	D$_{MaxBTV}$	N/A	17.25 (115% D$_{MeanBTV}$)	17.25 (115% D$_{MeanBTV}$)
BTV	Minimum D$_{99BTV}$	N/A	13.5 (90% D$_{MeanBTV}$)	13.5 (90% D$_{MeanBTV}$)
GTV1 − BTV	Minimum D$_{99GTV1 - BTV}$	N/A	9.6 (90% D$_{Mean}$)	9.6 (80% D$_{Mean}$)
GTV1 − BTV	D$_{MeanGTV - BTV}$	N/A	10.7	10.7
Gastrointestinal tract	D$_{Max}$ (Gy)	≤8	≤8	≤8
Spine	V$_{8 Gy}$ (%)	≤5	≤5	≤5

Note. GTV = gross tumor volume delineated on planning CT.

TABLE 4
ΔD between Prescribed and Planned Dose for GTV1, BTV and GTV1 – BTV for All Study Arms

Rat no.	Treatment type	GTV1 ΔD (mean ± SD) (Gy)	GTV1 $\Delta D_{95\%}/\Delta D_{5\%}$ (Gy)	BTV ΔD (mean ± SD) (Gy)	BTV $\Delta D_{95\%}/\Delta D_{5\%}$ (Gy)	GTV1 – BTV ΔD (mean ± SD) (Gy)	GTV1 – BTV $\Delta D_{95\%}/\Delta D_{5\%}$ (Gy)
1	Uniform	0.16 ± 0.11	0.02/0.37	N/A	N/A	N/A	N/A
2	Uniform	0.23 ± 0.16	0.02/0.53	N/A	N/A	N/A	N/A
3	Uniform	0.24 ± 0.14	0.04/0.49	N/A	N/A	N/A	N/A
4	BTV$_{high}$	0.98 ± 0.83	0.08/2.59	1.08 ± 0.68	0.12/2.24	0.94 ± 0.87	0.07/2.77
5	BTV$_{high}$	1.42 ± 1.04	0.14/3.68	0.98 ± 0.51	0.12/1.78	1.66 ± 1.17	0.15/3.98
6	BTV$_{high}$	0.89 ± 0.82	0.08/2.77	0.52 ± 0.37	0.06/1.26	1.11 ± 0.92	0.09/3.02
7	BTV$_{low}$	1.37 ± 1.17	0.07/3.74	0.41 ± 0.32	0.03/0.96	1.89 ± 1.13	0.21/3.95
8	BTV$_{low}$	1.14 ± 0.98	0.06/3.17	0.45 ± 0.57	0.03/1.24	1.44 ± 0.97	0.14/3.36
9	BTV$_{low}$	1.03 ± 1.10	0.05/3.42	0.39 ± 0.44	0.02/0.99	1.35 ± 1.18	0.10/3.59

Note. GTV = gross tumor volume delineated on planning CT; BTV = biological target volume delineated on pretreatment FDG PET.

penumbra) need to be taken into account. In particular when treating small GTVs and planning to deliver high-dose gradients within these GTVs, the BTV sizes need to be selected so that the gradients are delivered with acceptable accuracy. Moreover, large BTVs in relatively small tumors might imply very limited dose gradients with MV beams, due to the relatively large penumbras (*22, 29*). In this study, for the BTV fractional size we used 30% of the GTV, in line with the strategy tested in an FDG-PET-based dose painting trial, which is ongoing at our institution (*12*). This methodological study will serve as a foundation for future research on the *in vivo* effects of FDG-based dose painting in a rat tumor model. In similar studies it will be important to include treatment arms where either the FDG-high-uptake areas (BTV$_{high}$) or the FDG-low-uptake areas (BTV$_{low}$) are targeted with higher doses than the rest of the GTV (dose redistribution). The hypothesis being tested would be that boosting only the BTV$_{high}$ region would improve outcome. As the geometry of the BTV$_{low}$ can be different from that of the BTV$_{high}$ (in our experiments, we observed that BTV$_{low}$ often included the outer shell of the GTV, while BTV$_{high}$ most frequently encompassed the central part of the GTV), it was necessary to assess feasibility of planning and

accuracy of delivery also for this scenario in a specific way. In our study, important planning objectives and dose metrics, such as D_{min}, D_{mean}, $D_{95\%}$ for GTV and BTV, were reasonably fulfilled for all treatment arms. We proved that, in general, differences between planned and delivered dose metrics were <5% for both low- (GTV – BTV) and high- (BTV) dose regions. For the assessment of dosimetric accuracy, we employed the conventional 3%/2 mm dose difference/distance to agreement gamma criterion (*30*). This yielded high-passing rates (>98%) for both uniform and heterogeneous plans when TPS dose distributions calculated on CT or CBCT were compared with radiochromic film measurements. These results support the methodological validity of our approach in our experimental set-up and constitute an important foundation to build on for future studies.

Several studies have already proved the feasibility of planning and delivery of heterogeneous dose distributions derived from clinical PET images, even with VMAT technology (*9, 31–33*). Our study shows that planning and delivery of heterogeneous dose distributions is feasible also for relatively small targets such as rat tumors. We need to emphasize that if the imaging had been performed on a

TABLE 5
DVH Metrics for GTV1 and BTV for All CT Calculated Plans

Rat no.	Treatment type	GTV1 $D_{5\%}$ CT (Gy)	GTV1 $D_{5\%}$ CBCT (Gy)	GTV1$_{95\%}$ CT (Gy)	GTV1$_{95\%}$ CBCT (Gy)	BTV $D_{5\%}$ CT (Gy)	BTV $D_{5\%}$ CBCT (Gy)	GTV1 D_{mean} CT (Gy)	GTV1 D_{mean} CBCT (Gy)	GTV1 D_{min} CT (Gy)	GTV1 D_{min} CBCT (Gy)	BTV$_{mean}$ CT (Gy)	BTV$_{mean}$ CBCT (Gy)
1	Uniform	12.4	12.3	11.7	11.7	n/a	n/a	12.1	12.1	11.1	11.0	n/a	n/a
2	Uniform	12.5	12.6	11.9	12.0	n/a	n/a	12.2	12.3	10.8	11.0	n/a	n/a
3	Uniform	12.5	12.3	11.7	11.4	n/a	n/a	12.2	12.0	10.9	10.0	n/a	n/a
4	BTV$_{high}$ boost	16.7	16.4	10.1	10.0	17.2	16.9	12.4	12.3	9.3	9.3	15.4	15.2
5	BTV$_{high}$ boost	16.7	16.3	9.1	9.1	16.8	16.5	13.0	12.8	8.4	8.4	15.9	15.8
6	BTV$_{high}$ boost	15.6	15.4	9.9	9.7	15.8	15.6	12.8	12.6	9.2	8.9	15.1	14.9
7	BTV$_{low}$ boost	15.6	15.6	8.7	8.7	15.8	15.8	12.8	12.8	8.3	8.3	15.1	15.2
8	BTV$_{low}$ boost	15.3	15.3	9.2	9.2	15.5	15.5	12.3	12.3	8.7	8.7	14.8	14.9
9	BTV$_{low}$ boost	15.3	14.2	10.2	10.3	15.6	15.7	12.8	12.8	9.8	9.9	14.9	15.1

Note. GTV = gross tumor volume delineated on pretreatment (planning) CT; BTV = biological target volume delineated on pretreatment PET-CT; $D_{95\%}$ = minimum dose delivered to 95% of the volume; $D_{5\%}$ = minimum dose delivered to 5% volume.
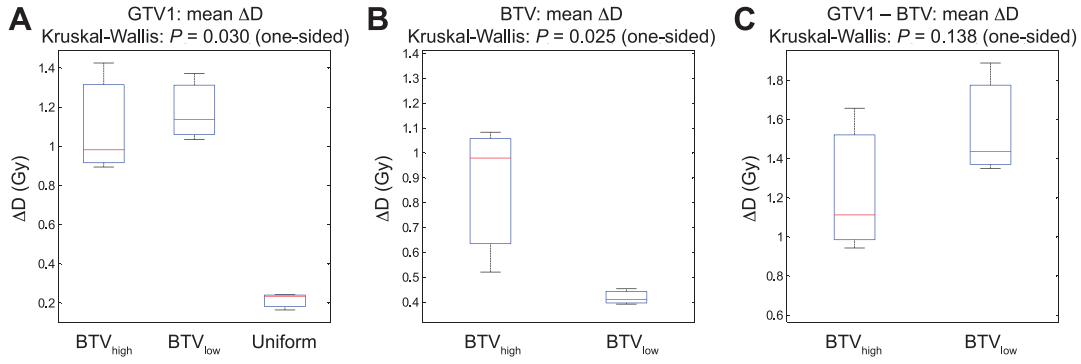
FIG. 3. Box and whiskers plots showing for absolute (per voxel) dose difference in GTV1 (panel A), BTV (panel B) and GTV1 – BTV (panel C) for each treatment group. The red line indicates for each structure and treatment arm the mean absolute (per voxel) dose difference between prescribed and achieved treatment planning system dose.
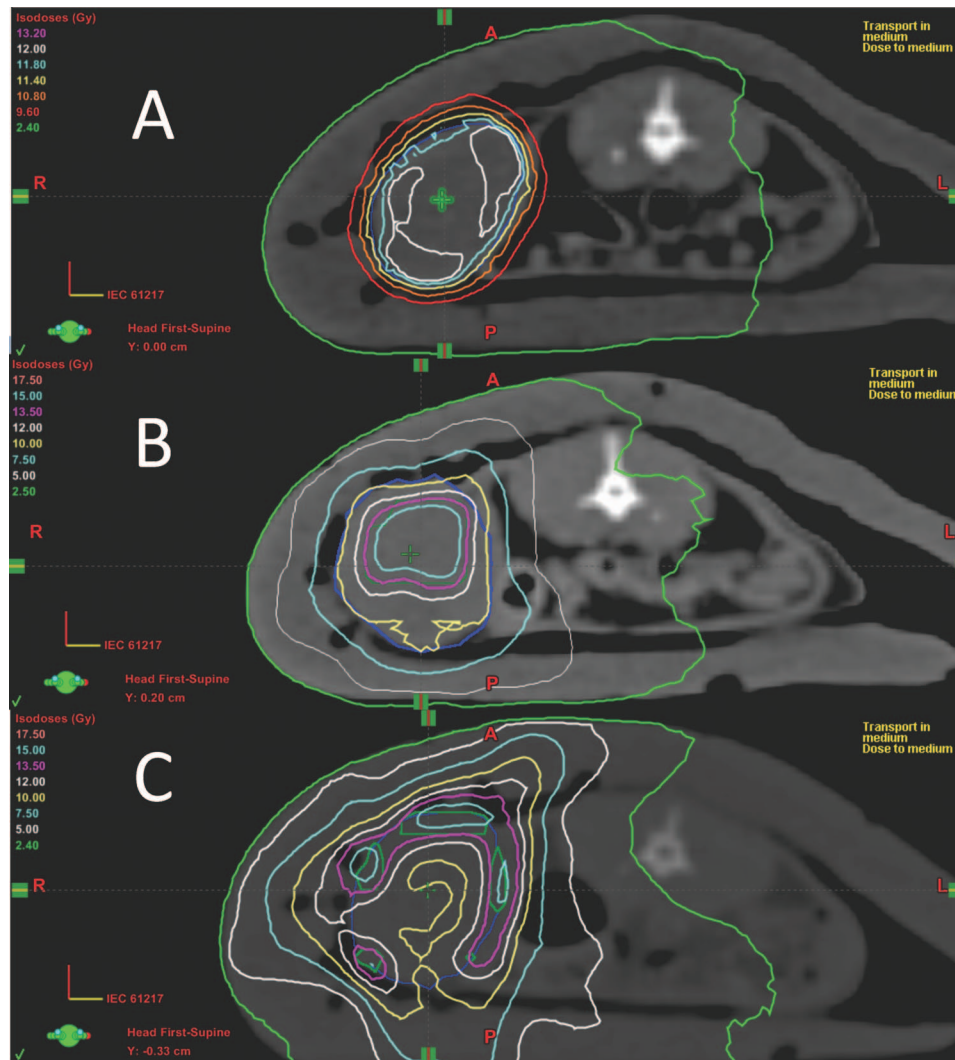

FIG. 4. Representative treatment plans for the three different arms of the study. Panel A: Dose distribution for a uniform plan (arm A) with a mean dose of 12 Gy prescribed to the GTV. Panel B: Dose distribution for an FDG high-uptake boost plan (BTV_high; arm B) with a prescribed dose of 15 Gy to 30% of the GTV with the highest FDG uptake. Panel C: Dose distribution for an FDG low-uptake boost plan (BTV_low; arm C) with a prescribed dose of 15 Gy to 30% of the GTV with the lowest FDG uptake.

TABLE 6
**Passing Rates for the Gamma Analyses of the 2D Dose Distributions for Verification Plans
Calculated in Eclipse on CT or CBCT Image against the Dose Distributions Measured by
Radiochromic Films for One Uniform and Three Heterogeneous Plans**

Rat no.	Treatment type	TPS CT D_{Max} (cGy)	Γ passing rate for CT RCF vs. TPS (%)	TPS CBCT D_{Max} (cGy)	Γ passing rate for CBCT RCF vs. TPS (%)
3	Uniform	12.7	99.2	13.0	98.8
4	BTV$_{high}$ boost	17.6	99.9	17.4	99.0
7	BTV$_{low}$ boost	16.4	98.25	16.4	98.9
9	BTV$_{low}$ boost	16.1	99.9	16.3	99.1

Notes. All γ analyses were performed with a dose difference/distance to agreement criterion of 3%/2 mm. Treatment planning system (TPS) doses were used as reference; RCF = radiochromic film.

µPET-CT imaging system it would be unlikely that one would have achieved the same level of accuracy for planning and delivery on a clinical VMAT system. To use the high-resolution information of the µPET-CT scanner the availability of a preclinical IMRT system will be indispensable.

By comparing the CT-planned dose distribution to the dose distribution recalculated on the online-matched CBCT, we assessed the ability to deliver the CT plans with satisfactory accuracy. In general, we found that the discrepancy between CT and CBCT dose metrics was within 2.5% and we could conclude that the planned dose distributions were delivered with acceptable accuracy upon good tumor matching.

In conclusion, we have developed a robust positioning and set-up verification protocol for PET-CT-based radiation dose painting studies in a rat rhabdomyosarcoma model using state-of-the-art clinical imaging and radiotherapy platforms. Our work also demonstrates the technical feasibility and the dosimetrical accuracy of this approach. Preclinical studies testing dose redistribution and dose escalation studies based on FDG uptake are ongoing in our laboratory. Although our study focused on FDG-PET uptake to identify potential radioresistant subvolumes (*12*), published data suggest that complementary imaging of hypoxia or drug uptake might lead to even more accurate selection of therapy-resistant BTVs than FDG uptake alone (*34–36*). We eagerly await more preclinical studies that are aimed at testing similar biological hypotheses and selecting promising dose painting strategies for future clinical trials.

SUPPLEMENTARY INFORMATION

Supplementary Methods. CT Hounsfield units (HU) to electron density (ED) data and CBCT calibration.
Figs. S1–S6.

ACKNOWLEDGMENTS

REFERENCES

1. Horsman MR, Mortensen LS, Petersen JB, Busk M, Overgaard J. Imaging hypoxia to improve radiotherapy outcome. Nat Rev Clin Oncol 2012; 9:674–87.

2. Marusyk A, Almendro V, Polyak K. Intra-tumour heterogeneity: a looking glass for cancer? Nat Rev Cancer 2012; 12:323–34.

3. Meijer TW, Kaanders JH, Span PN, Bussink J. Targeting hypoxia, HIF-1, and tumor glucose metabolism to improve radiotherapy efficacy. Clin Cancer Res 2012; 18:5585–94.

4. Komar G, Lehtio K, Seppanen M, Eskola O, Levola H, Lindholm P, et al. Prognostic value of tumour blood flow, [(18)F]EF5 and [(18)F]FDG PET/CT imaging in patients with head and neck cancer treated with radiochemotherapy. Eur J Nucl Med Mol Imaging 2014; 41:2042–50.

5. Ling CC, Humm J, Larson S, Amols H, Fuks Z, Leibel S, et al. Towards multidimensional radiotherapy (MD-CRT): biological imaging and biological conformality. Int J Radiat Oncol Biol Phys 2000; 47:551–60.

6. Lambin P, Petit SF, Aerts HJ, van Elmpt WJ, Oberije CJ, Starmans MH, et al. The ESTRO Breur Lecture 2009. From population to voxel-based radiotherapy: exploiting intra-tumour and intra-organ heterogeneity for advanced treatment of non-small cell lung cancer. Radiother Oncol 2010; 96:145–52.

7. Sovik A, Malinen E, Olsen DR. Strategies for biologic image-guided dose escalation: a review. Int J Radiat Oncol Biol Phys 2009; 73:650–8.

8. Bentzen SM, Gregoire V. Molecular imaging-based dose painting: a novel paradigm for radiation therapy prescription. Semin Radiat Oncol 2011; 21:101–10.

9. Thorwarth D, Alber M. Implementation of hypoxia imaging into treatment planning and delivery. Radiother Oncol 2010; 97:172–5.

10. Vanderstraeten B, Duthoy W, De Gersem W, De Neve W, Thierens H. [18F]fluoro-deoxy-glucose positron emission tomography ([18F]FDG-PET) voxel intensity-based intensity-modulated radiation therapy (IMRT) for head and neck cancer. Radiother Oncol 2006; 79:249–58.

11. Madani I, Duthoy W, Derie C, De Gersem W, Boterberg T, Saerens M, et al. Positron emission tomography-guided, focal-dose escalation using intensity-modulated radiotherapy for head and neck cancer. Int J Radiat Oncol Biol Phys 2007; 68:126–35.

12. van Elmpt W, De Ruysscher D, van der Salm A, Lakeman A, van

der Stoep J, Emans D, et al. The PET-boost randomised phase II dose-escalation trial in non-small cell lung cancer. Radiother Oncol 2012; 104:67–71.

13. Heukelom J, Hamming O, Bartelink H, Hoebers F, Giralt J, Herlestam T, et al. Adaptive and innovative radiation treatment for improving cancer treatment outcome (ARTFORCE); a randomized controlled phase II trial for individualized treatment of head and neck cancer. BMC Cancer 2013; 13:84.

14. Bentzen SM. Theragnostic imaging for radiation oncology: dose-painting by numbers. Lancet Oncol 2005; 6:112–7.

15. Butterworth KT, Prise KM, Verhaegen F. Small animal image-guided radiotherapy: status, considerations and potential for translational impact. Br J Radiol 2015; 88:20140634.

16. Verhaegen F, van Hoof S, Granton PV, Trani D. A review of treatment planning for precision image-guided photon beam pre-clinical animal radiation studies. Z Med Phys 2014; 24:323–34.

17. Peeters SG, Zegers CM, Lieuwes NG, van Elmpt W, Eriksson J, van Dongen GA, et al. A comparative study of the hypoxia PET tracers [F]HX4, [F]FAZA, and [F]FMISO in a preclinical tumor model. Int J Radiat Oncol Biol Phys 2015; 91:351–9.

18. Dubois LJ, Lieuwes NG, Janssen MH, Peeters WJ, Windhorst AD, Walsh JC, et al. Preclinical evaluation and validation of [18F]HX4, a promising hypoxia marker for PET imaging. Proc Natl Acad Sci U S A 2011; 108:14620–5.

19. Curtis SB, Tenforde TS. Assessment of tumour response in a rat rhabdomyosarcoma. Br J Cancer Suppl 1980; 4:266–70.

20. Landuyt W, Ahmed B, Nuyts S, Theys J, Op de Beeck M, Rijnders A, et al. In vivo antitumor effect of vascular targeting combined with either ionizing radiation or anti-angiogenesis treatment. Int J Radiat Oncol Biol Phys 2001; 49:443–50.

21. Low DA, Dempsey JF. Evaluation of the gamma dose distribution comparison method. Med Phys 2003; 30:2455–64.

22. Podesta M, Persoon LC, Verhaegen F. A novel time dependent gamma evaluation function for dynamic 2D and 3D dose distributions. Phys Med Biol 2014; 59:5973–85.

23. van Hoof SJ, Granton PV, Landry G, Podesta M, Verhaegen F. Evaluation of a novel triple-channel radiochromic film analysis procedure using EBT2. Phys Med Biol 2012; 57:4353–68.

24. Bentzen SM. Dose painting and theragnostic imaging: towards the prescription, planning and delivery of biologically targeted dose distributions in external beam radiation oncology. Cancer Treat Res 2008; 139:41–62.

25. Petit SF, Aerts HJ, van Loon JG, Offermann C, Houben R, Winkens B, et al. Metabolic control probability in tumour sub-volumes or how to guide tumour dose redistribution in non-small cell lung cancer (NSCLC): an exploratory clinical study. Radiother Oncol 2009; 91:393–8.

26. van Hoof SJ, Granton PV, Verhaegen F. Development and validation of a treatment planning system for small animal radiotherapy: SmART-Plan. Radiother Oncol 2013; 109:361–6.

27. Verhaegen F, Granton P, Tryggestad E. Small animal radiotherapy research platforms. Phys Med Biol 2011; 56:R55–83.

28. Humphries SM, Boyd K, Cornish P, Newman FD. Comparison of Super Stuff and paraffin wax bolus in radiation therapy of irregular surfaces. Med Dosim 1996; 21:155–7.

29. Clausen MM, Hansen AE, Af Rosenschold PM, Kjaer A, Kristensen AT, McEvoy FJ, et al. Dose escalation to high-risk sub-volumes based on non-invasive imaging of hypoxia and glycolytic activity in canine solid tumors: a feasibility study. Radiat Oncol 2013; 8:262.

30. Ezzell GA, Burmeister JW, Dogan N et al. IMRT commissioning: multiple institution planning and dosimetry comparisons, a report from AAPM Task Group 119. Med Phys 2009; 36:5359–73.

31. Thorwarth D, Eschmann SM, Paulsen F, Alber M. Hypoxia dose painting by numbers: a planning study. Int J Radiat Oncol Biol Phys 2007; 68:291–300.

32. Petit SF, Dekker AL, Seigneuric R, Murrer L, van Riel NA, Nordsmark M, et al. Intra-voxel heterogeneity influences the dose prescription for dose-painting with radiotherapy: a modelling study. Phys Med Biol 2009; 54:2179–96.

33. Thorwarth D, Geets X, Paiusco M. Physical radiotherapy treatment planning based on functional PET/CT data. Radiother Oncol 2010; 96:317–24.

34. De Ruysscher D, Kirsch CM. PET scans in radiotherapy planning of lung cancer. Radiother Oncol 2010; 96:335–8.

35. Kim Y, Tome WA. Dose-painting IMRT optimization using biological parameters. Acta Oncol 2010; 49:1374–84.

36. Chang JH, Wada M, Anderson NJ, Lim Joon D, Lee ST, Gong SJ, et al. Hypoxia-targeted radiotherapy dose painting for head and neck cancer using (18)F-FMISO PET: A biological modeling study. Acta Oncol 2013; 52:1723–9.